

Distinct Mechanisms Control Human Naive and Antigen-Experienced CD8⁺ T Lymphocyte Proliferation¹

Marco Migliaccio,*[‡] Pedro Miguel Sousa Alves,^{†‡} Pedro Romero,^{†‡} and Nathalie Rufer^{2*‡}

Human Ag-specific CD8⁺ T lymphocytes are heterogeneous and include functionally distinct populations. In this study, we report that at least two distinct mechanisms control the expansion of circulating naive, memory, and effector CD8⁺ T lymphocytes when exposed to mitogen or Ag stimulation. The first one leads to apoptosis and occurs shortly after *in vitro* stimulation. Susceptibility to cell death is prominent among primed T cell subsets, and it is inversely correlated with the size of the *ex vivo* Bcl-2^{high} population within these subsets. Importantly, the Bcl-2^{high} phenotype is associated to the proportion of responsive CD8⁺ T cells, independently of their differentiation stage. The second one depends on the expression of newly synthesized cyclin-dependent kinase inhibitor p16^{INK4a} that occurs in a significant fraction of T cells that had been actively cycling, leading to their cell cycle arrest upon stimulation. Strikingly, accumulation of p16^{INK4a} protein preferentially occurs in naive as opposed to primed derived T lymphocytes and is not related to apoptosis. Significant levels of p16 are readily detectable in a small number of *ex vivo* CD8⁺ T cells. Our observations reveal that activation-induced p16 expression represents an alternative process to apoptosis, limiting the proliferation potential of activated naive derived T lymphocytes. *The Journal of Immunology*, 2006, 176: 2173–2182.

Circulating CD8⁺ and CD4⁺ T lymphocytes are heterogeneous and composed of various subpopulations with distinct functional characteristics (1–3). The patterns of expression of cell surface markers such as CD45RA, CCR7, and CD27 have been widely used to distinguish and isolate human Ag-experienced CD8⁺ T lymphocytes from naive cells. Although naive T cells display a CD45RA⁺CCR7⁺CD27⁺ pattern, primed cells can be subdivided into at least three additional subsets. Central memory (CM)³ T cells (CD45RA⁻CCR7⁺CD27⁺) possess both high proliferative capacity and the ability to migrate to secondary lymph organs, but lack immediate cytolytic function. In contrast, effector memory (EM) T cells (CD45RA⁻CCR7⁻CD27^{+/−}) home preferentially to nonlymphoid tissues and produce variable levels of effector cytokines such as IFN- γ . Finally, differentiated E T cells (CD45RA⁺CCR7⁻CD27⁻) display low proliferative capacity and high levels of effector (E) molecules and cytotoxicity.

Human or mouse CD4⁺ and CD8⁺ T lymphocytes proliferate *ex vivo* when exposed to either mitogens or Ags. However, the response to stimulation is quite heterogeneous because about one-half of the cells enter into cell cycle, whereas the remainder of the cells fail to divide (4–7). Heterogeneity to mitogen or Ag responsiveness may be associated with Ag-experienced cells that have

undergone proliferation and differentiation, before their isolation *ex vivo*. Indeed, human naive and memory T cell subsets do present different capacities to proliferate in response to TCR stimulation or homeostatic cytokines (8, 9). What is unclear, at present, is the nature of the factors that control T lymphocyte proliferation and whether these can be differentially regulated in T cell subsets, and as a consequence, may lead to potential differences in their *in vivo* and *in vitro* proliferative capacity.

Apoptosis induced either by TCR triggering or cytokine deprivation has been shown to limit survival and replicative capacity of T cells (10). It involves mainly the engagement of surface death receptors such as Fas (11) or of a mitochondrially dependent pathway involving members of the Bcl-2 family (12). Several studies have shown that Bcl-2 expression plays a role in T cell survival (reviewed in Ref. 13). T cells that either overexpress the antiapoptotic protein Bcl-2 (14) or lack proapoptotic members of the Bcl-2 family such as Bim, Bak, or Bax seem to be protected from cell death (15, 16). Increased levels of Bcl-2 protein were reported in Ag-specific memory T cells during the chronic phase of viral infection when compared with those found among the E T cells of the acute phase (17, 18). Moreover, previous studies also showed that levels of Bcl-2 expression differed among human T cell subpopulations *ex vivo* (9, 19). However, the precise relationship among Bcl-2 expression levels, cell survival, and proliferation potential within naive, memory, and E CD8⁺ T cell subsets upon activation remains unclear.

Cell growth arrest and quiescence are maintained in cells by the retinoblastoma protein (pRb) family members that bind to and inhibit the transcriptional activity of E2F. Therefore, to enter into cell division cycle, the pRb proteins, especially pRb itself, must be inactivated by cyclin-dependent kinases (CDKs), through phosphorylation (20). Both pRb phosphorylation and concomitant entry into the cell cycle can be prevented by the presence of the p16^{INK4a} (hereafter p16) protein, a CDK inhibitor belonging to the INK4 family (21, 22). In mesenchymal and epithelial cells, the p16 protein is expressed in response to various forms of cell stress and is associated with irreversible cell cycle arrest (23–27).

The role and function of p16 in regulating T lymphocyte cell cycle progression remain intriguing. The relevance of p16 in regulating *in vivo* T cell proliferation is suggested by the high

*Swiss Institute for Experimental Cancer Research, Epalinges, Switzerland; [†]Division of Clinical Onco-Immunology, Ludwig Institute for Cancer Research, Lausanne Branch, University Hospital, Lausanne, Switzerland; and [‡]National Center of Competence in Research Molecular Oncology Program of the Swiss National Science Foundation, Epalinges, Switzerland

Received for publication September 23, 2005. Accepted for publication December 7, 2005.

The costs of publication of this article were defrayed in part by the payment of page charges. This article must therefore be hereby marked *advertisement* in accordance with 18 U.S.C. Section 1734 solely to indicate this fact.

¹ M.M., P.M.S.A. and, N.R. are supported by the National Center of Competence in Research Molecular Oncology, a research instrument of the Swiss National Science Foundation.

² Address correspondence and reprint requests to Dr. Nathalie Rufer, Swiss Institute for Experimental Cancer Research, 155 ch. des Boveresses, CH-1066 Epalinges, Switzerland. E-mail address: Nathalie.Rufer@isrec.ch

³ Abbreviations used in this paper: CM, central memory; 7-AAD, 7-aminoactinomycin D; CDK, cyclin-dependent kinase; E, effector; EM, effector memory; PD, population doubling; pRb, retinoblastoma protein.

frequency of loss of function mutations in the *p16* gene in T cell leukemias and lymphomas (reviewed in Ref. 28). Moreover, p16-deficient mice display enlarged thymus with significant increased cell numbers, and T splenocytes exhibit enhanced mitogen responsiveness, consistent with the established role of p16 in constraining cell proliferation (29). Recently, we reported that p16 expression could directly be induced as a consequence of T cell activation (7). Importantly, knocking down p16 expression allowed increased proliferation of T cells. Our data further indicate that accumulation of p16 is responsible for the exit of a significant proportion of CD8⁺ T cells from the proliferative population, thus limiting their numerical expansion in vitro. Interestingly, detectable p16 accumulation was restricted to a variable proportion of the cultured cells. At present, a critical issue involves the identity of the subset of CD8⁺ T cells (if not all) that expresses the p16 protein.

In this study, we report a kinetic analysis of the proliferative response of purified CD8⁺ T cell subsets upon activation with mitogens or specific antigenic peptides. We show that Bcl-2^{high} expression represents a surrogate marker to estimate the proportion of responsive T cells. The fraction of responding cells, although variable for each subset, gradually diminishes upon cell differentiation. Importantly, a large fraction of naive derived CD8⁺ T lymphocytes expresses high levels of p16 protein in response to stimulation, and this expression is coincident with reduced rates of proliferation. Our results indicate striking differences in the control of the expansion potential between human CD8⁺ T cell subpopulations.

Materials and Methods

Monoclonal Abs

The following mAbs were purchased from BD Pharmingen: anti-CD27 FITC and PE, anti-p16 PE, anti-Bcl-2 PE, purified anti-CCR7 rat IgG, goat anti-rat IgG allophycocyanin, and anti-CD8 allophycocyanin/Cy7. Anti-CD45RA PE-Texas Red mAb was obtained from Beckman Coulter. Synthesis of allophycocyanin-labeled HLA-A2*0201/Melan-A₂₆₋₃₅ (ELAGIGILTV) and HLA-A2*0201/Flu matrix protein₅₈₋₆₆ (GILGFVFTL) multimers was performed, as previously described (30).

Cell preparation and cell sorting by flow cytometry

Peripheral blood samples were collected from healthy volunteers ($n = 11$; average, 33 years; range, 27–38 years), with a normal proportion of CD8⁺ T lymphocytes (average, 23%; range, 15–35%). Four elderly individuals were further included in the ex vivo p16 expression study (average, 68 years; age range, 61–75 years). PBMCs were obtained by density centrifugation using Ficoll-Hypaque (Pharmacia). CD8⁺ T lymphocytes were positively purified from fresh PBMCs using anti-CD8-coated magnetic microbeads (MACS; Miltenyi Biotec). Cells were stained with anti-CD8, anti-CCR7, anti-CD45RA, and anti-CD27 Ab and sorted into naive (CD8⁺CD45RA⁺CCR7⁺CD27⁺), CM (CD8⁺CD45RA⁻CCR7⁺CD27⁺), EM (CD8⁺CD45RA⁻CCR7⁻CD27^{+/−}), and E (CD8⁺CD45RA⁺CCR7⁻CD27⁻) T subpopulations on a FACS Vantage SE using CellQuest software (BD Biosciences). Immediate reanalysis of the isolated T cell subsets revealed >95% purity. Melan-A- and Flu-specific T lymphocytes were stained with either allophycocyanin-labeled Melan-A or Flu multimers for 1 h at room temperature.

Cell culture

Cultures of human T cell subsets were obtained following flow cytometry-based cell sorting of 0.5×10^5 to 2×10^5 cells, seeded in culture plates in RPMI 1640 medium supplemented with 8% human serum and 150 U/ml human rIL-2 (a gift from GlaxoSmithKline), and stimulated with 1 μ g/ml PHA (Sodiag) plus 1×10^6 /ml irradiated allogeneic PBMCs (3000 rad) as feeder cells. Most importantly, cells were seeded at the same concentration per well whether T cells were derived from naive, CM, EM, or E subsets. In particular, the volume of medium and the concentration of feeder cells were adapted to the initial number of sorted cells. Cell density per well was further kept similar for each derived T cell subculture, following the second and third rounds of stimulation. Growing cells were always maintained between 0.5 and 2×10^6 cells/ml, upon daily care. Medium was renewed, and cell cultures were split whenever required. The stimulation procedure

was repeated every 12 days of culture (31). Population doublings (PD) were determined by periodic counting of living cells using trypan blue to exclude dying cells, and according to the following formula: PD (day x ; day y) = $(\log(\text{average cell count at day } y) - \log(\text{average cell seeded at day } x))/\log_2$. To allow the direct comparison of the proliferative potential of each subset, the PD at day 5 after stimulation was adjusted to the initial fraction of cells that start to proliferate in response to stimulation based on Fig. 1D as corrected PD = (PD at day 5/percentage of recruited cells) \times 100. The rate of proliferation (PD/day) was calculated for each time point (day x ; day y) as PD (day x ; day y)/(day y - day x).

For the expansion of Ag-specific T cells from PBMCs, 0.2×10^5 cells/well were cultivated in RPMI 1640 medium complemented with 8% human serum, in 96-well round-bottom plates, in the presence of either Melan-A (10 μ M) or Flu (10 μ M) peptide. Human rIL-2 (1000 U/ml) was added after 2 days, and fresh medium from day 3 onward. Microcultures were pooled on day 12 before FACS analysis. In the second cycle of stimulation, 10^6 Ag-specific T cells were then cocultured with 0.3×10^5 irradiated peptide-pulsed T2 cells (10,000 rad) plus 1 μ g/ml β_2 -microglobulin (Fluka).

When indicated, cell samples were resuspended in 1 ml of CFSE (Molecular Probes) solution (2 μ g/ml in PBS), incubated for 10 min at 37°C, washed twice, and seeded into 24-well plates. The percentage of cells that responded to mitogen stimulation at day 5 was calculated using the area of every single CFSE dilution peak, as described by Wells et al. (4).

Annexin V staining, intracellular staining, and flow cytometry analysis

To enumerate living, apoptotic, and necrotic T cells at 36 h after stimulation, cells were washed, resuspended in annexin V buffer, and stained with Cy-5-conjugated annexin V (BD Biosciences) and 7-aminoactinomycin D (7-AAD; BD Biosciences), according to manufacturer instructions. Allogeneic PBMCs (CFSE negative) were discarded by gating the cells in the corresponding plots. Bcl-2 and p16 expression was assessed after fixation and permeabilization with Cytofix/Cytoperm buffer (BD Biosciences) for 15 min, and staining with PE-conjugated mAbs against human Bcl-2, p16, or corresponding isotype-matched control mAbs. Cells were incubated 1 h at room temperature, washed with washing buffer (BD Biosciences), resuspended in 400 μ l of PBS/3% FCS/0.05% NaN₃, and kept at 4°C until analyzed on a FACSCalibur flow cytometer (BD Biosciences). Mean fluorescence intensity values for Bcl-2 expression were obtained by subtracting the geometric mean value of the isotype control histogram from that of the anti-Bcl-2 histogram. The percentage of p16-positive cells was determined, as recently described (7).

BrdU incorporation assay

For BrdU incorporation studies, 10^6 cell samples were incubated in the presence of 10 μ g/ml BrdU during the indicated periods of time at 37°C. Cells were then fixed, permeabilized, treated with DNase to expose BrdU epitopes, and stained with an anti-BrdU Ab and 7-AAD using the BrdU flow kit (BD Biosciences). When indicated, anti-p16 Ab or the corresponding isotype control was also added for simultaneous intracellular staining.

Statistics

The results were analyzed by Student's *t* test and by linear regression analysis.

Results

Mitogen-stimulated human CD8⁺ T cell subsets display different proliferation potential depending on their ex vivo differentiation status

To investigate the precise dynamics of cell proliferation within various CD8⁺ T cell subsets, we conducted a quantitative flow cytometry analysis of the proliferative response to mitogen using CFSE labeling as an indicator of cell division. Subsets of CD8⁺ T cells isolated by flow cytometry sorting from peripheral blood were CFSE labeled, and their response to mitogens was analyzed over a period of 7 days (Fig. 1). Naive and CM CD8⁺ T cell subsets underwent massive expansion when compared with EM and E T cell subpopulations. Importantly, the proportion of cells that did not initiate cell division was significantly higher in the EM and E T cell subsets, as observed at days 3 and 5 after stimulation (Fig. 1, A and B). By day 7, all undivided cells (CFSE^{high}), comprising as well EM- and E-derived T cells, were diluted out, most

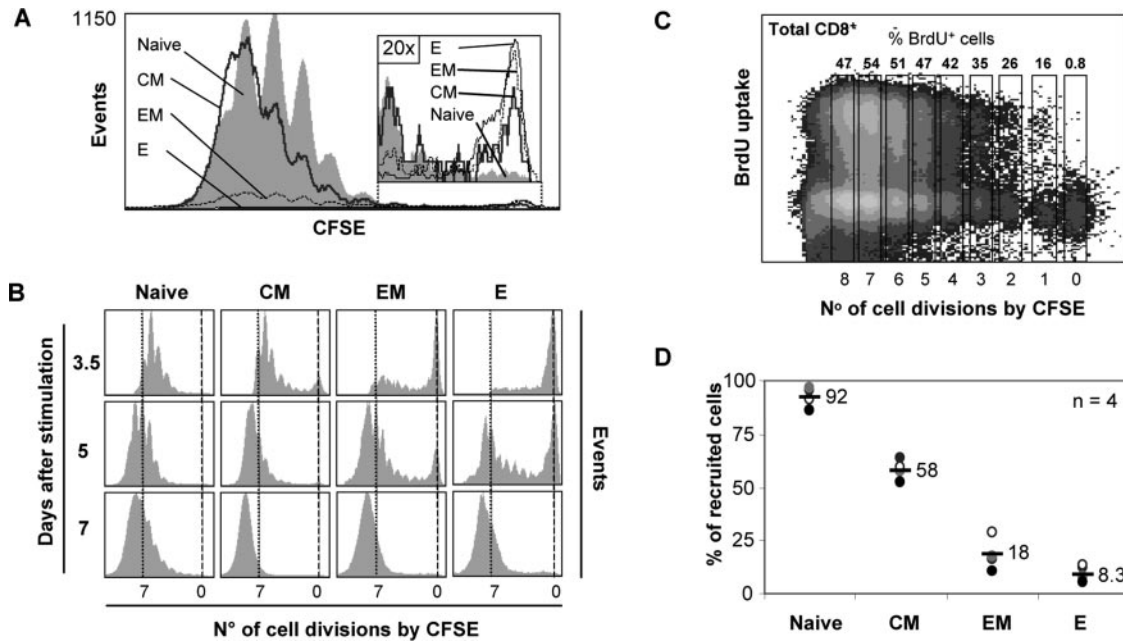


FIGURE 1. Expansion potential of human CD8⁺ T cell subsets following mitogen stimulation. Naive, CM, EM, and E CD8⁺ T cells were FACS sorted according to their expression of CD45RA, CCR7, and CD27; stained with CFSE; and stimulated. *A*, Overlays of the CFSE fluorescence histograms (identical scale) obtained separately from each T cell subset at day 5 after stimulation. Progeny from identical numbers of precursors were analyzed allowing direct comparison between samples. A 20-fold image amplification of the CFSE analysis (corresponding to the highest fluorescence peak) is depicted. *B*, CFSE fluorescence histograms at days 3.5, 5, and 7 after stimulation, normalized according to the highest peak of fluorescence. Dotted lines indicate CFSE intensity corresponding to undivided cells (*right*) and cells that underwent seven cell divisions (*left*). *C*, Mitogen-stimulated and CFSE-labeled bulk CD8⁺ T lymphocytes were incubated during 1 h in the presence of BrdU on day 5 after stimulation. The proportion of cycling BrdU⁺ cells according to the magnitude of the CFSE fluorescent signal (the corresponding number of cell divisions is indicated in the *x*-axis) is depicted. Of note, T cells that had divided at least four times (CFSE^{low}) are composed of highly cycling cells (50% BrdU⁺). *D*, The percentage of cells, within each subset, that start to proliferate in response to mitogen stimulation was calculated according to the CFSE fluorescence profiles (*B*), as previously described (4). Mean of four independent experiments.

likely because of the high cycling rate up to seven to eight divisions of the activated cells.

Using BrdU incorporation assays, we next measured the fraction of CD8⁺ T cells that was in, or entered into, the S phase of the cell cycle during a 1-h pulse at day 5 following stimulation (Fig. 1C). Clearly, all T cells incorporating BrdU were composed of cells that had divided one to eight times (CFSE^{low}). In contrast, <1% of the CFSE^{high} cells were able to uptake BrdU directly, indicating that these cells could no longer be recruited into cell cycle. Based on this observation, the proportion of cells, within each CD8⁺ T cell subset, that start to proliferate in response to mitogen stimulation was then assessed according to the obtained area of every single CFSE dilution peak (Fig. 1B), as previously described (4) (Fig. 1D). Strikingly, while almost all naive T cells started to divide in response to stimulation (mean \pm SD; 92 \pm 4%), there was a progressive and marked decline in the proportion of primed T cells that were recruited to proliferate, from CM (52 \pm 5%) through EM (18 \pm 8%) to E (8 \pm 3%) T cells. Similar analyses on blood samples collected from four different healthy individuals provided highly reproducible results (Fig. 1D). Although a small proportion of E T cells (<10%) did divide in response to mitogen, their cycling rates were similar to those of naive or CM CD8⁺ T cells. This is best illustrated by the similar number of CFSE dilution peaks, from one up to eight cell divisions, observed in all proliferating CD8⁺ T cell subsets (Fig. 1B).

Together, these results show that the heterogeneity in mitogen responsiveness detected on the entire CD8 population in fact reflects the different proportion of cells, within each T cell subset, that respond to mitogens. Furthermore, the fraction of responding cells is highly associated to the *ex vivo* differentiation status of

human CD8⁺ T lymphocytes, from naive through CM to EM and E cells.

*High levels of Bcl-2 protein expression in T cell subsets *ex vivo* correlate with resistance to apoptosis and mitogen responsiveness*

Activation of T lymphocytes through the TCR stimulates cell proliferation, but may also induce apoptosis. Thus, the low proliferative potential of Ag-experienced T lymphocytes could be associated with a high rate of cell death following stimulation. To address this issue, we determined the proportion of cells undergoing apoptosis in each *ex vivo* isolated T cell subset, shortly after mitogen stimulation, by simultaneous annexin V and 7-AAD costaining (Fig. 2A). Apoptotic cells were only rarely found within cells of naive origin, with most of the cells remaining alive following 36 h of stimulation (90%). In contrast, there was a progressive and marked increase in the proportion of early (annexin V⁺ 7-AAD⁻) and late (annexin V⁺ 7-AAD⁺) apoptotic cells, from CM to EM and E T cell subset. These data were extended when annexin V and 7-AAD costaining was combined with the CFSE dilution analysis at day 5 after stimulation (Fig. 2B). Importantly, most of the undivided CFSE^{bright} cells consisted of cells that underwent apoptosis (annexin V⁺ 7-AAD⁺).

To further explore the relationship between the fraction of cells that is susceptible to apoptosis and those cells that are recruited into cell cycle, we characterized the expression of the antiapoptotic Bcl-2 protein within each CD8⁺ T cell subset (Fig. 2C). All cycling cells (CFSE^{low}), whether they were derived from naive or primed T cell subsets, revealed high levels of Bcl-2 expression at day 4 after stimulation. In addition, there was a strong positive

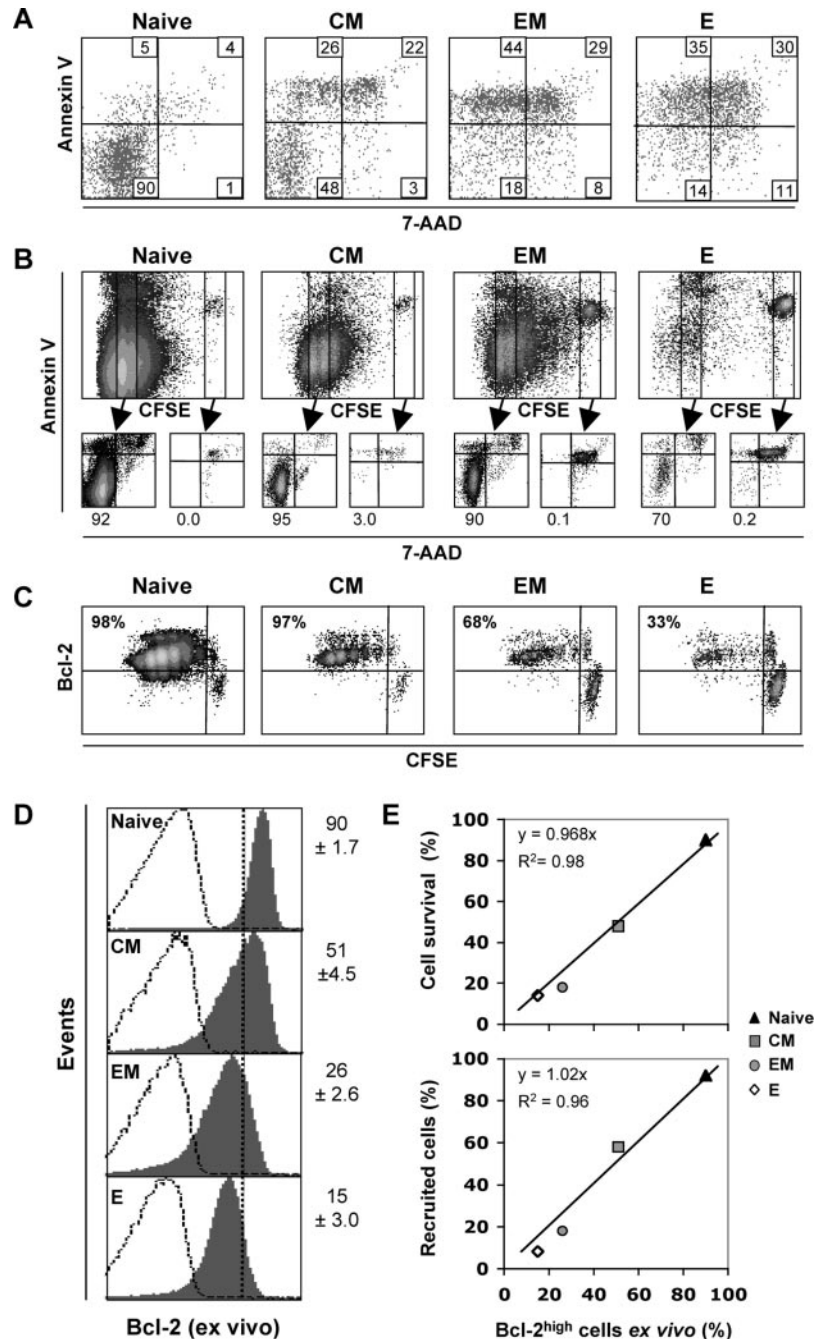


FIGURE 2. Positive correlation among Bcl-2^{high} expression, cell survival, and mitogen responsiveness in human CD8⁺ T cell subsets. *A*, Simultaneous staining with annexin V (AV) and 7-AAD at 36 h after stimulation allows the quantification (in percentages) of living (AV⁻/7AAD⁻), early apoptotic (AV⁺/7AAD⁻), late apoptotic (AV⁺/7AAD⁺), and necrotic (AV⁻/7AAD⁺) cells. One representative experiment of three is shown. *B*, Dot plots representing simultaneous staining with CFSE, annexin V, and 7-AAD at day 5 after stimulation are shown for each T cell subset. Percentage of living cells (AV⁻/7AAD⁻) is depicted for CFSE^{low} and CFSE^{bright} gated cells. *C*, Simultaneous CFSE and Bcl-2 staining at day 4 after stimulation is shown for each T cell subset. *D*, Ex vivo purified CD8⁺ T cells were stained for the expression of CD45RA, CCR7, and CD27; fixed; permeabilized; and stained for Bcl-2 expression. Both isotype control (open) and Bcl-2 (gray) histograms are depicted. Mean ± SD (in percentage) of four independent experiments. As maximal differential expression of Bcl-2 was observed between naive and differentiated E T cells, this allowed us to set a well-defined cutoff point for ex vivo Bcl-2^{high}-expressing cells. Note that high and homogeneous Bcl-2 fluorescence was typically observed in naive T cells. *E*, Positive correlation between the proportion of ex vivo Bcl-2^{high}-expressing cells with cell survival (percentage of living AV⁻/7AAD⁻ cells at 36 h) and with the fraction of cells that start to proliferate (see Fig. 1*D*) within all four T cell subsets.

correlation between the proportion of ex vivo Bcl-2^{high}-expressing cells present within all four T cell subsets (Fig. 2*D*), with 1) cell survival at 36 h after stimulation ($R^2 = 0.98$) as well as with 2) the fraction of cells that responded to mitogen ($R^2 = 0.96$) (Fig. 2*E*). Thus, our observations suggest that high levels of Bcl-2 protein expression (ex vivo Bcl-2^{high} phenotype) in T cells may be predictive of the population of cells that will respond and enter into cell cycle upon mitogen stimulation, regardless of their differentiation stage. Moreover, the size of the ex vivo Bcl-2^{high} population is variable in each studied T cell subset, ranging from 90% in the naive derived cells to <15% in E T lymphocytes.

Ex vivo stimulated naive and primed CD8⁺ T lymphocytes are characterized by distinct growth kinetics

To define more precisely the growth kinetics of CD8⁺ T cell subsets, we determined the proliferative rate of ex vivo sorted naive

and primed T cells by counting living cells at regular intervals after mitogen stimulation (Fig. 3). Of note, the cell density was kept similar for each cell culture whether cells derived from naive or primed sorted T cell subsets (see *Material and Methods*). During the first 5 days of in vitro culture, naive and CM sorted T cells underwent extensive proliferation, as both subsets recruited a higher proportion of cells into cell cycle (Fig. 1*D*). To allow the direct comparison between each proliferating subset, the cell yields were adjusted to the initial fraction of cells that start to proliferate in response to stimulation (see corrected PD; Fig. 3*A*). Surprisingly, a significant decline in the PD and thus in the proliferative rate was found for the naive T cell subset from day 6 onward. In contrast, Ag-experienced T cells maintained a steady rate of proliferation over 3 additional days of culture (until day 9; Fig. 3*A*). These findings were made with cells obtained during the first cycle of mitogenic stimulation of T cell subsets ex vivo. When we

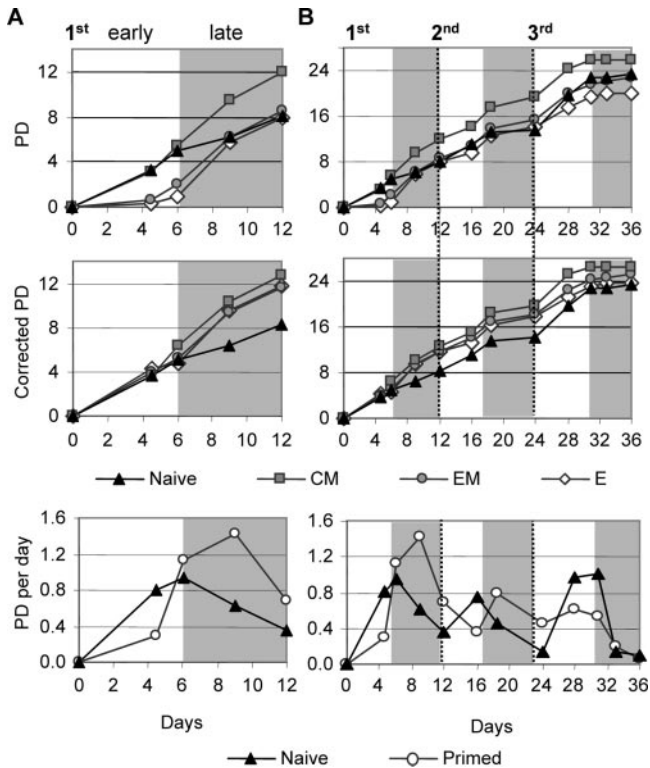


FIGURE 3. Growth kinetics of human CD8⁺ T cell subsets after mitogen stimulation. CD8⁺ T cell subsets were isolated by cell sorting and mitogen stimulated. Their growth kinetic was assessed by periodic cell counting (PD) following the first cycle of stimulation (A) as well as two consecutive stimulation cycles (second and third; B). PD, corrected PD, and rate of proliferation (PD/day) were calculated, as described in *Materials and Methods*. Rate of proliferation of naive vs primed (average of CM, EM, and E) T cells is depicted. Mean of four (A) and two (B) independent experiments. SD <10% of mean value (data not shown). Each cycle of stimulation is divided into early (open) and late (gray) phase.

assessed the proliferation potential of the individual T cell subsets in two consecutive stimulation cycles, the same reproducible pattern was observed in each cycle (Fig. 3B). Thus, our data describe distinct growth kinetics between naive and Ag-experienced T cells, best illustrated by a two-phase model. During the early phase of mitogen stimulation, naive derived cells exhibit faster rate of proliferation over the one found in EM and E T lymphocytes (days 0–6). There is, however, a complete reversion in growth kinetics during the late phase of stimulation, with sustained proliferation primarily found within the primed derived T subsets (days 6–12).

Naive, but not primed, derived T lymphocytes express high levels of p16 protein, associated to cell cycle arrest

We recently reported that the expression of the cyclin-dependent kinase inhibitor p16 limits the proliferative potential of CD8⁺ T lymphocytes responding to mitogen stimulation by preventing a fraction of cells to enter into cell cycle (7). We next addressed whether de novo p16 expression is associated with the transient decline in the proliferative rate observed in naive derived T lymphocytes during the late phase of every stimulation cycle (Fig. 3), by determining p16 expression levels by intracellular staining. High levels of p16 were found in a substantial proportion of naive derived T cells, while only in small proportions of primed T cell subsets (Fig. 4A). This increase in p16 expression became particularly robust from day 12 onward, and >50% of the naive-derived T population contained high amounts of p16 by day 24 after

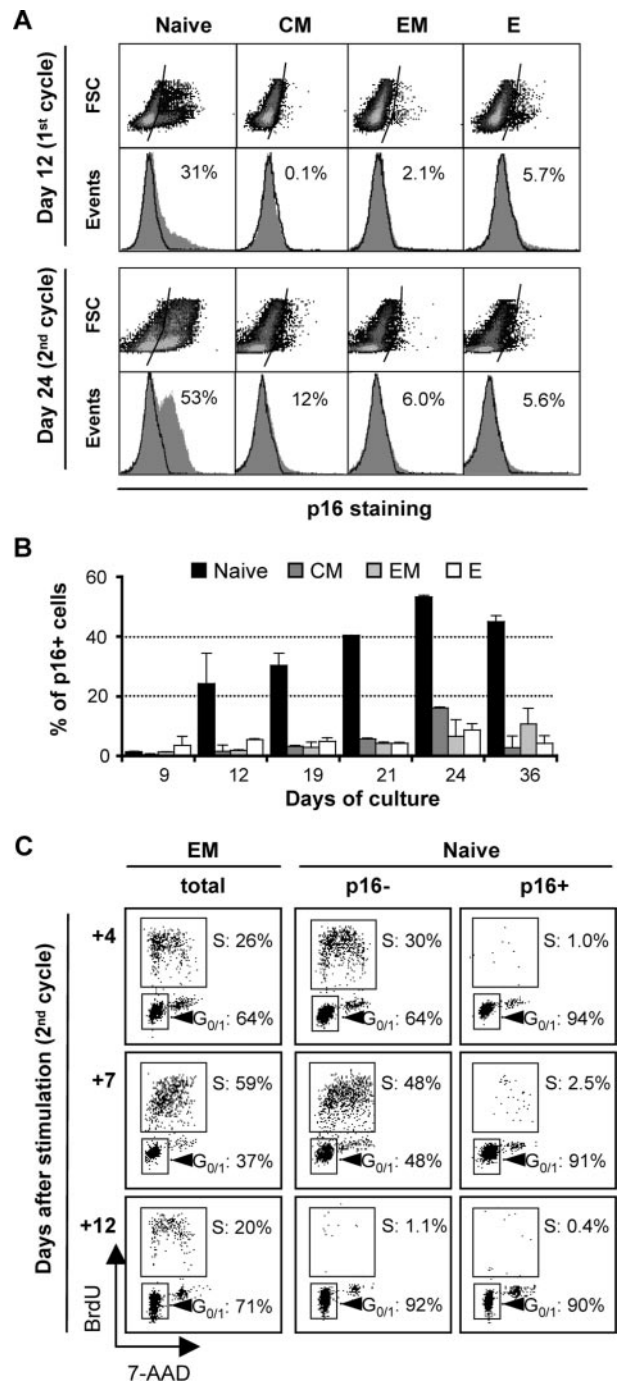


FIGURE 4. Expression of p16 protein in human CD8⁺ T cell subsets following repeated rounds of stimulation and during cell cycle replication. CD8⁺ T cell subsets were isolated by cell sorting and mitogen stimulated. Levels of p16 expression were measured at various time points over three cycles of stimulation. A, Representative dot plots and histograms were obtained at days 12 and 24 after stimulation. The reference for p16 positivity is based on the signal obtained with an isotype control Ab (see solid line). Both isotype control (open) and p16 (gray) histograms are depicted. B, The percentage of p16-positive cells was calculated, as described in *Materials and Methods*. Data collected from two independent experiments are expressed as mean ± SD. C, BrdU incorporation (1-h pulse) and DNA content (7-AAD; linear scale) analysis on gated p16-negative and p16-positive naive derived T cells as well as on total EM-derived T cells at days 4, 7, and 12 (second cycle of stimulation). The proportion (in percentages) of T cells, respectively, in G₀-G₁ (see arrow; BrdU⁻) and in S (BrdU⁺) phases of cell cycle is shown. The EM subpopulation is representative of all primed (CM, EM, and E) T cells.

stimulation (Fig. 4B). Moreover, similar levels of p16 expression were found when CD8⁺ T lymphocytes were stimulated in the absence of exogenous IL-2, indicating a limited impact, if not any of this cytokine on the induction of p16 protein (data not shown). These p16-positive T cells were predominantly composed of non-cycling cells, as assessed by BrdU incorporation assays and simultaneous 7-AAD costaining of the DNA content (Fig. 4C). Collectively, our data show that activation-induced p16 expression is responsible in preventing a fraction of cells to enter into cell cycle when stimulated. Accumulation of p16 protein occurs preferentially in cultured T lymphocytes derived from naive, but not from primed, subpopulations. Because parameters such as cell density and medium consumption were, for each derived T cell subset culture, tightly controlled during stimulation (see *Material and Methods*), this differential induction of p16 is unlikely to be explained by inadequate culture conditions (32). Of note, the percentage of cycling cells within the naive derived compartment was barely detectable at day 12 after stimulation, in comparison with the one present in primed derived T cells (Fig. 4C). These results further support our previous observations that almost all naive derived T cells exit the cell cycle during the late phase of the stimulation cycle (Fig. 3). They also indicate that cell cycle arrest may be mediated by either the p16 protein or by other yet-to-be-defined mechanisms.

Activation-induced p16 expression is not related to apoptosis and is a delayed response of some naive derived T lymphocytes to mitogen stimulation

To investigate the precise kinetics of apoptosis and activation-induced p16 expression, we measured annexin V and p16 expression in bulk CD8⁺ T lymphocytes on days 4, 7, and 10 after the second cycle of stimulation (Fig. 5). Although an increase in annexin V-positive cells was detected 4 days after stimulation, this percentage of positive cells decreased thereafter, presumably as a result of the increase in the number of proliferating cells. In contrast, the p16 expression kinetics in cells was delayed, with an augmentation of p16-expressing cells from day 5–6 onward (Fig. 5) (7). Virtually no cells were positive for both p16 and annexin V, and apoptotic and p16-positive cells showed markedly different forward/side light scatter profiles. Most annexin V-positive cells were smaller

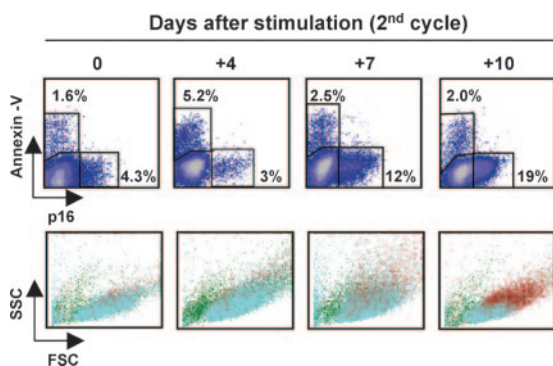


FIGURE 5. Apoptosis and activation-induced p16 expression kinetics in bulk CD8⁺ T cells following mitogen stimulation. Dot plots representing simultaneous staining with annexin V and anti-p16 of bulk CD8⁺ T cell populations at each indicated number of days after the second cycle of stimulation. *Insets*, Represent either annexin V- or p16-positive cell percentages. The setting for p16-positive cells is based on the isotype control staining. Optical scattering profiles of the same cell populations showing p16⁺ cells (red dots), annexin V⁺ cells (green dots), and double-negative cells (blue dots). Note that very low percentage of analyzed cells presented a double-positive phenotype (<1%).

than the rest of the population (green dots), with shrinkage being a typical feature of apoptotic cells. p16-positive cells (red dots), while partially overlapping in size with the proliferating cells (blue dots), were on average larger and had slightly increased cytoplasmic granularity. These observations nicely correlated to the morphological changes, in regard to cell volume and loss of original shape, found in mesenchymal and epithelial cells (33). Undoubtedly, cells undergoing apoptosis were distinct from cells that expressed p16 after several rounds of cell division. Altogether, our results demonstrate that apoptosis primarily involves primed T cells during the early phase of stimulation. In contrast, activation-induced p16 expression is a delayed response affecting mainly cells of naive origin during the late phase of stimulation.

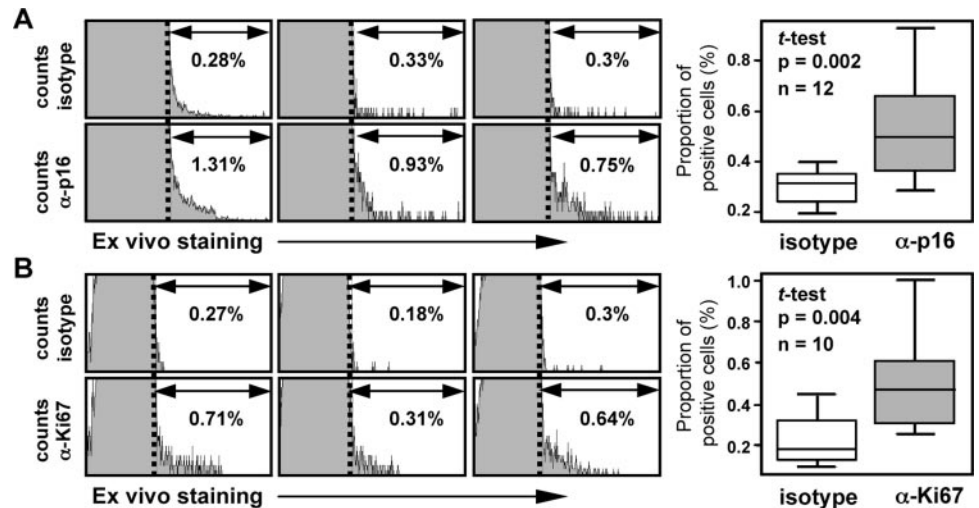
Detectable frequencies of p16-expressing CD8⁺ T lymphocytes ex vivo

We observed that p16 expression could be induced in response to mitogen stimulation *in vitro*, and that its expression in T cells was associated to cell cycle arrest. An important question raised from our observations is whether the proliferative potential of T cells *in vivo*, particularly of recently activated cells, might to some extent be controlled by p16/pRb pathway. To address this technically challenging point, we have analyzed the expression of p16 *ex vivo* in freshly isolated bulk CD8⁺ T lymphocytes collected from 12 healthy individuals by flow cytometry (Fig. 6A). We found low, but significantly detectable levels of p16 in a small fraction of circulating CD8⁺ T cells (mean \pm SD; 0.53 \pm 0.21%, $p < 0.005$). Because *ex vivo* primary T cells only expressed minute amounts of the p16 protein, we could neither address which phenotypic subset specifically expressed the protein, nor whether these cells have increased size and granularity, as do the *in vitro* generated ones (Fig. 5). In parallel experiments, we performed an intracellular staining for Ki67 content, a nuclear Ag mostly present in cycling cells (Fig. 6B). Similarly to p16 expression, a small proportion of *ex vivo* isolated CD8⁺ T lymphocytes expressed low, but readily detectable levels of Ki67 (mean \pm SD; 0.5 \pm 0.22%, $p < 0.005$). These data are in line with the view that most mature T cells isolated from peripheral blood are found in a quiescent resting state, and consequently, only low proportions of either p16-expressing cells or cycling cells (34) are to be expected.

Apoptosis and activation-induced p16 expression distinctly control the proliferation potential of Ag-stimulated Melan-A- and Flu-specific CD8⁺ T lymphocytes

The findings described above were made with T cells obtained from naive and primed subpopulations following stimulation with the mitogenic lectin PHA. To address whether apoptosis and activation-induced p16 expression also occurred after antigenic stimulation, we monitored the expansion of Melan-A- and Flu-specific CD8⁺ T cells activated by the cognate Ag. The majority of circulating Melan-A_{26–35}-specific T cells from HLA-A2 healthy donors are phenotypically and functionally naive despite their high frequency. In contrast, influenza (matrix protein_{58–66})-specific cells display a functional memory status (35). Significant expansions of Ag-specific T cells, resulting in up to 40% of the CD8⁺ T cell population, were obtained after a single round of Ag/IL-2 stimulation (day 12, Fig. 7A). The levels of Bcl-2 were relatively higher within the Melan-A-specific subpopulations than among the Flu-derived T cells. Once stimulated by the Ag, Flu-specific T lymphocytes in contrast to Melan-A-specific cells had a higher propensity to cell death, and, as a consequence, a lower proportion of such cells entered cell division (Fig. 7B). Thus, similar to bulk CD8⁺ T cell subsets, Ag-specific T cells derived from cells that

FIGURE 6. p16 and Ki-67 expression in circulating CD8⁺ T lymphocytes ex vivo. Freshly isolated purified CD8⁺ T cells were fixed, permeabilized, and stained for either p16 (A) or Ki67 (B) expression. Representative p16 or Ki67 staining of three healthy donors, including respective isotype control histograms, is depicted. Box plot of isotype⁺/p16⁺ (A; *n* = 12) and isotype⁺/Ki67⁺ (B; *n* = 10) cells in CD8⁺ T cells from healthy individuals. For the p16 staining, each donor sample was tested in duplicate. Of note, as it is yet not feasible to perform a costaining of p16 together with Ki67, we could not assess whether Ki67-positive cells were also p16 negative.



had been primed in vivo showed increased susceptibility to apoptosis following antigenic stimulation. Conversely, while more resistant to apoptosis, a large fraction of Melan-A-, but not Flu-specific T cells accumulated high levels of p16 protein from days 12 to 24 after Ag stimulation (Fig. 7C). Because Melan-A-specific cells are entirely composed of ex vivo naive derived lymphocytes (35), our data nicely confirm experiments performed on the total naive T cell subset (Fig. 4). These results indicate that apoptosis and activation-induced p16 expression differentially regulate the proliferative potential of naive and primed derived T lymphocytes not only in response to mitogen, but also to Ag stimulation.

Discussion

In the present study, we show that the proliferative potential of human CD8⁺ T lymphocytes is restricted by at least two distinct and unrelated processes. The first one occurs shortly after stimulation and involves programmed cell death. In contrast, the second one depends on the activation-induced p16 expression and follows delayed kinetics, as a result of de novo synthesis of the p16 protein in response to stimulation. Although susceptibility to apoptosis increases progressively among Ag-experienced T cells (CM→EM→E), p16 protein expression predominantly involves cells derived from the naive T cell pool. Importantly, both apoptosis and p16 expression processes do also limit the expansion of Melan-A- and Flu-specific CD8⁺ T cells activated by the cognate Ag (Fig. 7).

Human CD8⁺ T lymphocytes isolated from peripheral blood are predominantly small quiescent cells in G₀-G₁ arrest of the cell cycle. CD8⁺ T cells stimulated with Ag or mitogen follow a binary fate: responsive cells (CFSE^{low}BrdU⁺) that start to proliferate, and nonresponsive cells (CFSE^{high}BrdU⁻) that do not. Most of the cells that are recruited into cell cycle express high levels of the antiapoptotic factor Bcl-2 (Fig. 2), as well as the activation-associated marker CD69 (data not shown). In contrast, the majority of cells not recruited into cell cycle undergo apoptosis by 36 h after stimulation. The work reported in this study confirms and further extends recent findings (9) that the capacity of T cells to proliferate in response to stimulation is associated with resistance to cell death and ex vivo Bcl-2 expression (Fig. 2). Strikingly, our observations indicate that each T cell subset, even differentiated E T lymphocytes, contains a population of cells ex vivo expressing high levels of the Bcl-2 protein (Bcl-2^{high} phenotype). Importantly, the Bcl-2^{high} phenotype is highly correlative with both enhanced rate of survival and mitogen responsiveness of T cells, regardless of their

differentiation stage. Numerous studies have shown that Bcl-2 has antiapoptotic effects; however, high levels of Bcl-2 also correlated with decreased proliferation, when using Bcl-2 overexpressing transgenic mice (36). In this study, we observed that actively dividing cells expressed high amounts of the Bcl-2 protein (Fig. 2). Thus, at least in our stimulation setting, the physiological Bcl-2^{high} expression levels do not seem to prevent proliferation of human cells. The size of the ex vivo Bcl-2^{high} population is, however, variable for each T cell subset and gradually declines with cell differentiation. The differential expression of the Bcl-2^{high} phenotype found within various CD8⁺ T cell subsets provides a rational explanation for the heterogeneous response to mitogen and Ag previously reported in bulk cultures of T lymphocytes (4–7). Finally, high Bcl-2 expression and cell survival can be significantly promoted in all derived T cell subsets by the presence of exogenous IL-7 cytokine (data not shown).

Another interesting finding is that, while the size of the Bcl-2^{high} pool of CD8⁺ T cells is progressively smaller with cell differentiation, from naive (90%) through CM (51%) to EM (26%) and E (15%) T cells, it is remarkably well maintained in different healthy individuals. What determines and preserves the given size of the Bcl-2^{high} population present in every subset, and within different donors? Bcl-2 expression can be induced by γ -chain signaling cytokines, e.g., IL-7 and IL-15 (10). One possibility is that the resource availability of homeostatic cytokines may favor the survival of naive and CM T cell subpopulations over differentiated EM and E T cells (37). Naive T cells bear functional receptors for IL-4 and IL-7, but not for IL-2 and IL-15 (reviewed in Ref. 10), whereas high expression of IL-15R has been reported in memory T cell subsets (9). Alternatively, yet unknown intrinsic factor(s) that is dependent of the lymphocyte differentiation state may directly control and maintain the relative size of the Bcl-2^{high} pool of CD8⁺ T cells.

Several studies, including ours, provide compelling evidence that the levels of Bcl-2 expression ex vivo are down-regulated in E T cells, both in human (9, 18, 19) and during acute infection of mice with lymphocytic choriomeningitis virus (17). These observations lend support to the notion that the high susceptibility to cell death, and consequently the low expansion potential in vitro and in vivo, is an intrinsic feature of differentiated E cells. However, in the latter report, Grayson et al. (17) also show that CD8⁺ memory T cells express higher levels of Bcl-2 than naive cells, suggesting that increased Bcl-2 expression is involved in the long-term maintenance of memory cells in vivo. Intriguingly, these results do not

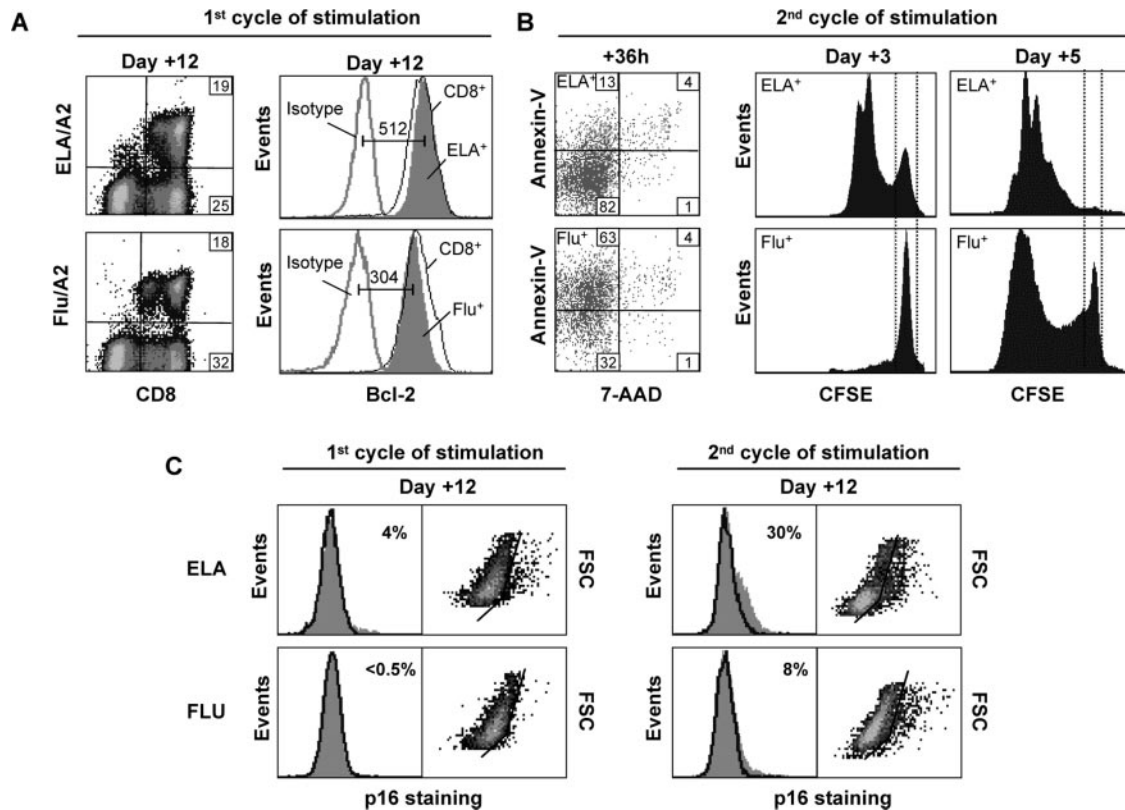


FIGURE 7. Bcl-2 expression, cell survival, mitogen responsiveness, and p16 expression in Ag-stimulated Melan-A- and Flu-specific T lymphocytes. *A*, Expansion of naive or memory CD8⁺ T cells from PBMCs following one round of stimulation with peptide and IL-2 (ELA/ELAGILTV (10 μ M) or Flu/GILGFVFTL (10 μ M)). Percentages of multimer staining cells and CD8⁺ T cells were obtained after 12 days of expansion, from one representative donor of three. Levels of Bcl-2 expression were measured within ELA- and Flu-specific CD8⁺ T lymphocytes by intracellular staining at day 12 (gray histograms) and normalized, as described in *Materials and Methods*. *B*, Following the second cycle of stimulation with peptide-pulsed T2 cells, Ag-specific T cells were assessed for the presence of apoptotic cells (at 36 h by annexin V and 7-AAD costaining) and their proliferative expansion (at days 3 and 5 by CFSE staining). *C*, Representative dot plots and histograms of p16 expression were obtained at days 12 after the first and second stimulation. The setting for p16-positive cells is based on the isotype control staining (solid line). One representative experiment of two is shown.

exactly recapitulate those obtained in humans (9, 19), in which levels of Bcl-2 protein, in particular the size of the Bcl-2^{high} population, are consistently found reduced in memory T cells (CM and EM cells; Fig. 2). To date, we do not have a rational explanation for the apparent contradictory findings concerning the differential role of Bcl-2 in naive and memory T lymphocytes derived from different mammalian organisms.

A major finding in this study is that the expression of the CDK inhibitor, p16, does not uniformly occur in all T lymphocytes, but selectively appears in a fraction of naive derived cells that had been activated and recruited into cell cycle upon stimulation *in vitro* (Fig. 4). These data extend our recent observations on bulk CD8⁺ T cells showing that p16-expressing cells are descendants of actively cycling p16-negative cells (7). Therefore, their p16 expression can only be the result of *de novo* synthesis of this protein, explaining the delayed kinetics observed in response to stimulation (Fig. 5). We also report a direct link between p16 expression and cell cycle arrest, because: 1) p16-expressing cells are found exclusively within G₀-G₁ phase of the cell cycle (Fig. 4), and 2) knocking down p16 expression by small interfering RNAs allows increased proliferation of T cells (7). Of note, the G₀-G₁ cell cycle arrest induced following p16 expression has been associated with morphological changes (33) and with irreversible growth arrest in fibroblasts and mammary epithelial cells (26). These observations and ours are consistent with the view that this G₀-G₁ cell cycle arrest state should be distinguished from the one described in quiescent mature T lymphocytes from peripheral blood. Altogether,

this study demonstrates that activation-induced p16 expression is a distinct process unrelated to apoptosis, regulating the proliferative potential of activated naive origin T lymphocytes in response to stimulation. Our results also point to T cell differentiation as a central program in regulating the expression of two functionally antagonist factors: the prosurvival Bcl-2 and the procell arrest p16. Naive T cells have the unique capability to express high levels of both proteins, resulting in resistance to apoptosis, but susceptibility to G₁ cell arrest. Conversely, differentiated memory and E T lymphocytes progressively down-regulate Bcl-2 expression, thus becoming susceptible to programmed cell death.

One question raised by our findings concerns the mechanisms underlying p16 up-regulation in a fraction of naive derived T cells following Ag or mitogen stimulation. There is some evidence that p16 appearance can be induced by stress due to inadequate tissue culture conditions (24). This has mostly been described in epithelial cells, and the resulting growth arrest is referred to as stress-induced senescence (reviewed in Ref. 32). Although one cannot formally exclude that inappropriate culture conditions contribute to the expression of p16 in cultured T lymphocytes, it is unlikely because all CD8⁺ T cell subsets were grown under the same conditions. Together, our observations point to an intrinsic mechanism that leads to p16 expression and, as a consequence, limits the proliferative potential of a fraction of activated naive origin T cells. Thus, beside its well-characterized tumor suppressor function, p16 may play an additional physiological role in limiting lymphocyte expansion *in vitro* and *in vivo*. Several arguments reinforce this

conclusion. First, mice lacking p16 have enhanced thymocyte (29) and splenocyte (47) expansion. Second, forced expression of p16 in thymocytes blocks T cell differentiation at the immature CD4⁻CD8⁻ stage without affecting the development of $\gamma\delta$ T cells (38). Finally, using single cell intracellular staining techniques, we show that low, but readily detectable levels of p16 can be observed in freshly isolated ex vivo CD8⁺ T lymphocytes (Fig. 6) (7). Because most mature T lymphocytes are in a quiescent state, it is expected that only very low frequencies of p16-expressing cells were to be found in the peripheral blood of healthy individuals. Thus, it is of great importance to further explore whether such expression is present in T lymphocytes isolated from draining lymph nodes, at the site of T cell activation, or in individuals during primary infection with, e.g., CMV, EBV, HIV, or influenza viruses.

What remains intriguing, at present, is why are mostly naive, but not primed T cells affected by p16 upon stimulation in vitro? In this regard, Veiga-Fernandes and Rocha (39) recently reported that mouse CD8⁺ memory T lymphocytes are maintained by elevated levels of D cyclins and CDK6 in a preactivated state, suggesting that they require a lower threshold of stimulation to enter the cell cycle than naive cells. In line with these observations, a comparative microarray analysis revealed differential expression of cell cycle regulatory genes that control the transition between G₁ and S phase in virus-specific CD8⁺ T cells (40, 41). In addition, the entry or exit of T cells from the cell cycle may also be determined by the levels of the classical cell cycle progression inhibitors, such as p27^{Kip1} and p16. Consistently, the levels of p27^{Kip1}, a member of the Cip/Kip family, were particularly high in freshly isolated naive CD8⁺ T lymphocytes from mice (39) and humans (data not shown). However, in contrast to p27^{Kip1}, p16 expression is almost undetectable in resting G₀-G₁ T cells ex vivo (Fig. 6), but is inducible upon in vitro stimulation (Fig. 4). Hence, our data would be in line with the hypothesis that p16 protein may be expressed as a consequence of the process of lymphocyte activation.

Because neither Fas nor TNF- α receptors are expressed in naive T cells, apoptosis via both ligands is unlikely to be involved (reviewed in Ref. 10). Moreover, when stimulated, only a small fraction of naive T cells, in contrast to Ag-experienced cells, undergoes programmed cell death (Fig. 2). Collectively, we propose that the proliferative expansion of recently activated naive T cells might be controlled by p16/pRb pathway in vivo. If some cells receive suboptimal signals (42), subsequent p16 expression may arrest cells in G₁, potentially leading to cellular senescence (43). Thus, activation-induced p16 expression may represent an alternative pathway to apoptosis, in controlling T lymphocyte expansion upon antigenic priming. The molecular mechanisms underlying senescence, in contrast to the signaling pathways leading to apoptosis, are only poorly understood (reviewed in Ref. 33). Upon entering the state of senescence, cells undergo a plethora of changes in morphology with increased cell volume and loss of original shape, accompanied by irreversible structural alterations in the nuclear heterochromatin (44). Whether senescence occurs in vivo is still a matter of debate (33). Nevertheless, a recent report provides, for the first time, convincing data that senescence may represent a biological mechanism that operates in cells in vivo (45).

At present, p16 monitoring may be foreseen as a new parameter to the design of optimal in vitro stimulation conditions (46) and future therapeutic application. Moreover, understanding the role of p16 protein and its direct effect in promoting G₁ cell arrest in naive T lymphocytes has potential implications for the optimization of vaccine-based therapeutic strategies against infection or cancer.

Acknowledgments

We are thankful to Dr. Daniel Speiser for critically reading the manuscript, and Dr. Immanuel Lüscher and Philippe Guillaume for synthesis of multimers. We thank Estelle Devereux for cell sorting and Patricia Corthésy-Henrioud for excellent technical assistance.

Disclosures

The authors have no financial conflict of interest.

References

- Hamann, D., P. A. Baars, M. H. Rep, B. Hooibrink, S. R. Kerkhof-Garde, M. R. Klein, and R. A. van Lier. 1997. Phenotypic and functional separation of memory and effector human CD8⁺ T cells. *J. Exp. Med.* 186: 1407–1418.
- Sallusto, F., D. Lenig, R. Förster, M. Lipp, and A. Lanzavecchia. 1999. Two subsets of memory T lymphocytes with distinct homing potentials and effector functions. *Nature* 401: 708–712.
- Rufer, N., A. Zippelius, P. Batard, M. J. Pittet, I. Kurth, P. Corthésy, J. C. Cerottini, S. Leyvraz, E. Roosnek, M. Nabholz, and P. Romero. 2003. Ex vivo characterization of human CD8⁺ T subsets with distinct replicative history and partial effector functions. *Blood* 102: 1779–1787.
- Wells, A. D., H. Gudmundsdottir, and L. A. Turka. 1997. Following the fate of individual T cells throughout activation and clonal expansion: signals from T cell receptor and CD28 differentially regulate the induction and duration of a proliferative response. *J. Clin. Invest.* 100: 3173–3183.
- Wells, A. D., M. C. Walsh, D. Sankaran, and L. A. Turka. 2000. T cell effector function and energy avoidance are quantitatively linked to cell division. *J. Immunol.* 165: 2432–2443.
- Zand, M. S., B. J. Briggs, A. Bose, and T. Vo. 2004. Discrete event modeling of CD4⁺ memory T cell generation. *J. Immunol.* 173: 3763–3772.
- Migliaccio, M., K. Raj, O. Menzel, and N. Rufer. 2005. Mechanisms that limit the in vitro proliferative potential of human CD8⁺ T lymphocytes. *J. Immunol.* 174: 3335–3343.
- Geginat, J., F. Sallusto, and A. Lanzavecchia. 2001. Cytokine-driven proliferation and differentiation of human naive, central memory, and effector memory CD4⁺ T cells. *J. Exp. Med.* 194: 1711–1719.
- Geginat, J., A. Lanzavecchia, and F. Sallusto. 2003. Proliferation and differentiation potential of human CD8⁺ memory T-cell subsets in response to antigen or homeostatic cytokines. *Blood* 101: 4260–4266.
- Marrack, P., and J. Kappler. 2004. Control of T cell viability. *Annu. Rev. Immunol.* 22: 765–787.
- Alderson, M. R., T. W. Tough, T. Davis-Smith, S. Braddy, B. Falk, K. A. Schooley, R. G. Goodwin, C. A. Smith, F. Ramsdell, and D. H. Lynch. 1995. Fas ligand mediates activation-induced cell death in human T lymphocytes. *J. Exp. Med.* 181: 71–77.
- Hildeman, D. A., Y. Zhu, T. C. Mitchell, J. Kappler, and P. Marrack. 2002. Molecular mechanisms of activated T cell death in vivo. *Curr. Opin. Immunol.* 14: 354–359.
- Vander Heiden, M. G., and C. B. Thompson. 1999. Bcl-2 proteins: regulators of apoptosis or of mitochondrial homeostasis? *Nat. Cell Biol.* 1: E209–E216.
- Strasser, A., A. W. Harris, and S. Cory. 1991. *bcl-2* transgene inhibits T cell death and perturbs thymic self-censorship. *Cell* 67: 889–899.
- Wei, M. C., W. X. Zong, E. H. Cheng, T. Lindsten, V. Panoutsakopoulou, A. J. Ross, K. A. Roth, G. R. MacGregor, C. B. Thompson, and S. J. Korsmeyer. 2001. Proapoptotic BAX and BAK: a requisite gateway to mitochondrial dysfunction and death. *Science* 292: 727–730.
- Hildeman, D. A., Y. Zhu, T. C. Mitchell, P. Bouillet, A. Strasser, J. Kappler, and P. Marrack. 2002. Activated T cell death in vivo mediated by proapoptotic *bcl-2* family member *bim*. *Immunity* 16: 759–767.
- Grayson, J. M., A. J. Zajac, J. D. Altman, and R. Ahmed. 2000. Cutting edge: increased expression of Bcl-2 in antigen-specific memory CD8⁺ T cells. *J. Immunol.* 164: 3950–3954.
- Dunne, P. J., J. M. Faint, N. H. Gudgeon, J. M. Fletcher, F. J. Plunkett, M. V. Soares, A. D. Hislop, N. E. Annels, A. B. Rickinson, M. Salmon, and A. N. Akbar. 2002. Epstein-Barr virus-specific CD8⁺ T cells that re-express CD45RA are apoptosis-resistant memory cells that retain replicative potential. *Blood* 100: 933–940.
- Akbar, A. N., N. Borthwick, M. Salmon, W. Gombert, M. Bofill, N. Shamsadeen, D. Pilling, S. Pett, J. E. Grundy, and G. Janosy. 1993. The significance of low *bcl-2* expression by CD45RO T cells in normal individuals and patients with acute viral infections: the role of apoptosis in T cell memory. *J. Exp. Med.* 178: 427–438.
- Grana, X., J. Garriga, and X. Mayol. 1998. Role of the retinoblastoma protein family, pRB, p107 and p130 in the negative control of cell growth. *Oncogene* 17: 3365–3383.
- Shapiro, G. I., C. D. Edwards, and B. J. Rollins. 2000. The physiology of p16^{INK4A}-mediated G₁ proliferative arrest. *Cell Biochem. Biophys.* 33: 189–197.
- Lea, N. C., S. J. Orr, K. Stoerber, G. H. Williams, E. W. Lam, M. A. Ibrahim, G. J. Muftic, and N. S. Thomas. 2003. Commitment point during G₀→G₁ that controls entry into the cell cycle. *Mol. Cell. Biol.* 23: 2351–2361.
- Alcorta, D. A., Y. Xiong, D. Phelps, G. Hannon, D. Beach, and J. C. Barrett. 1996. Involvement of the cyclin-dependent kinase inhibitor p16^{INK4a} in replicative senescence of normal human fibroblasts. *Proc. Natl. Acad. Sci. USA* 93: 13742–13747.

24. Ramirez, R. D., C. P. Morales, B. S. Herbert, J. M. Rohde, C. Passons, J. W. Shay, and W. E. Wright. 2001. Putative telomere-independent mechanisms of replicative aging reflect inadequate growth conditions. *Genes Dev.* 15: 398–403.
25. De Magalhaes, J. P., F. Chainiaux, J. Remacle, and O. Toussaint. 2002. Stress-induced premature senescence in BJ and hTERT-BJ1 human foreskin fibroblasts. *FEBS Lett.* 523: 157–162.
26. Beausejour, C. M., A. Krtolica, F. Galimi, M. Narita, S. W. Lowe, P. Yaswen, and J. Campisi. 2003. Reversal of human cellular senescence: roles of the p53 and p16 pathways. *EMBO J.* 22: 4212–4222.
27. Naka, K., A. Tachibana, K. Ikeda, and N. Motoyama. 2004. Stress-induced premature senescence in hTERT-expressing ataxia telangiectasia fibroblasts. *J. Biol. Chem.* 279: 2030–2037.
28. Drexler, H. G. 1998. Review of alterations of the cyclin-dependent kinase inhibitor INK4 family genes p15, p16, p18 and p19 in human leukemia-lymphoma cells. *Leukemia* 12: 845–859.
29. Sharpless, N. E., N. Bardeesy, K. H. Lee, D. Carrasco, D. H. Castrillon, A. J. Aguirre, E. A. Wu, J. W. Horner, and R. A. DePinho. 2001. Loss of p16^{Ink4a} with retention of p19^{Arf} predisposes mice to tumorigenesis. *Nature* 413: 86–91.
30. Romero, P., P. R. Dunbar, D. Valmori, M. Pittet, G. S. Ogg, D. Rimoldi, J. L. Chen, D. Lienard, J. C. Cerottini, and V. Cerundolo. 1998. Ex vivo staining of metastatic lymph nodes by class I major histocompatibility complex tetramers reveals high numbers of antigen-experienced tumor-specific cytolytic T lymphocytes. *J. Exp. Med.* 188: 1641–1650.
31. Lamers, C. H., R. J. van de Griend, E. Braakman, C. P. Ronteltap, J. Benard, G. Stoter, J. W. Gratama, and R. L. Bolhuis. 1992. Optimization of culture conditions for activation and large-scale expansion of human T lymphocytes for bispecific antibody-directed cellular immunotherapy. *Int. J. Cancer* 51: 973–979.
32. Shay, J. W., and I. B. Roninson. 2004. Hallmarks of senescence in carcinogenesis and cancer therapy. *Oncogene* 23: 2919–2933.
33. Ben-Porath, I., and R. A. Weinberg. 2004. When cells get stressed: an integrative view of cellular senescence. *J. Clin. Invest.* 113: 8–13.
34. Douek, D. C., M. R. Betts, B. J. Hill, S. J. Little, R. Lempicki, J. A. Metcalf, J. Casazza, C. Yoder, J. W. Adelsberger, R. A. Stevens, et al. 2001. Evidence for increased T cell turnover and decreased thymic output in HIV infection. *J. Immunol.* 167: 6663–6668.
35. Zippelius, A., M. J. Pittet, P. Batard, N. Rufer, M. de Smedt, P. Guillaume, K. Ellefsen, D. Valmori, D. Lienard, J. Plum, et al. 2002. Thymic selection generates a large T cell pool recognizing a self-peptide in humans. *J. Exp. Med.* 195: 485–494.
36. Cheng, N., Y. M. Janumyan, L. Didion, C. Van Hofwegen, E. Yang, and C. M. Knudson. 2004. Bcl-2 inhibition of T-cell proliferation is related to prolonged T-cell survival. *Oncogene* 23: 3770–3780.
37. Freitas, A. A., and B. Rocha. 2000. Population biology of lymphocytes: the flight for survival. *Annu. Rev. Immunol.* 18: 83–111.
38. Lagresle, C., B. Gardie, S. Eyquem, M. Fasseu, J. C. Vieville, M. Pla, F. Sigaux, and J. C. Bories. 2002. Transgenic expression of the p16^{Ink4a} cyclin-dependent kinase inhibitor leads to enhanced apoptosis and differentiation arrest of CD4⁺CD8⁺ immature thymocytes. *J. Immunol.* 168: 2325–2331.
39. Veiga-Fernandes, H., and B. Rocha. 2004. High expression of active CDK6 in the cytoplasm of CD8 memory cells favors rapid division. *Nat. Immunol.* 5: 31–37.
40. Kaech, S. M., S. Hemby, E. Kersh, and R. Ahmed. 2002. Molecular and functional profiling of memory CD8 T cell differentiation. *Cell* 111: 837–851.
41. Latner, D. R., S. M. Kaech, and R. Ahmed. 2004. Enhanced expression of cell cycle regulatory genes in virus-specific memory CD8⁺ T cells. *J. Virol.* 78: 10953–10959.
42. Gett, A. V., F. Sallusto, A. Lanzavecchia, and J. Geginat. 2003. T cell fitness determined by signal strength. *Nat. Immunol.* 4: 355–360.
43. Hayflick, L., and P. S. Moorhead. 1961. The serial cultivation of human diploid cell strains. *Exp. Cell Res.* 25: 585–621.
44. Narita, M., S. Nunez, E. Heard, A. W. Lin, S. A. Hearn, D. L. Spector, G. J. Hannon, and S. W. Lowe. 2003. Rb-mediated heterochromatin formation and silencing of E2F target genes during cellular senescence. *Cell* 113: 703–716.
45. Schmitt, C. A., J. S. Fridman, M. Yang, S. Lee, E. Baranov, R. M. Hoffman, and S. W. Lowe. 2002. A senescence program controlled by p53 and p16^{Ink4a} contributes to the outcome of cancer therapy. *Cell* 109: 335–346.
46. Maus, M. V., B. Kovacs, W. W. Kwok, G. T. Nepom, K. Schlienger, J. L. Riley, D. Allman, T. H. Finkel, and C. H. June. 2004. Extensive replicative capacity of human central memory T cells. *J. Immunol.* 172: 6675–6683.
47. Bianchi, T., N. Rufer, R. H. MacDonald, and M. Migliaccio. The tumor suppressor p16^{Ink4a} regulates T lymphocyte survival. *Oncogene*. In press.